Mixed quadrature lattice Boltzmann models for the simulation of the circular Couette flow using the vielbein formalism

Sergiu Busuioc and Victor E. Ambruș

Departement of Physics, West University of Timișoara
Bd. Vasile Pârvan 4, 300223 Timișoara, Romania

DSFD 2017, 13/07/2017

Outline

- Boltzmann equation with respect to arbitrary coordinates system
- Boltzmann equation with respect to orthonormal vielbein fields
- Gauss-Hermite quadrature
- Circular Couette flow: Shear flows between coaxial cylinders
    - Rigid rotation
    - Hydrodynamic, transition and ballistic flow regimes

Boltzmann equation

- Evolution equation of the one-particle distribution function f with respect to the Cartesian coordinates:

$$\frac{\partial f}{\partial t} + \frac{p^i}{m}\frac{\partial f}{\partial x^i} + F^i \frac{\partial f}{\partial p^i} = J[f]. \tag{1}$$

- Hydrodynamic moments of order N give macroscopic quantities:

$N = 0$:	number density:	$n = \int d^3p\, f,$
$N = 1$:	velocity:	$\mathbf{u} = \frac{1}{nm}\int d^3p\, f\, \mathbf{p},$
$N = 2$:	temperature:	$T = \frac{2}{3n}\int d^3p\, f\, \frac{\boldsymbol{\xi}^2}{2m}, \qquad (\boldsymbol{\xi} = \mathbf{p} - m\mathbf{u}),$
$N = 3$:	heat flux:	$\mathbf{q} = \frac{1}{2m^2}\int d^3p\, f\, \boldsymbol{\xi}^2\, \boldsymbol{\xi}.$

Cartesian grid and momentum space decomposition along the Cartesian axes.

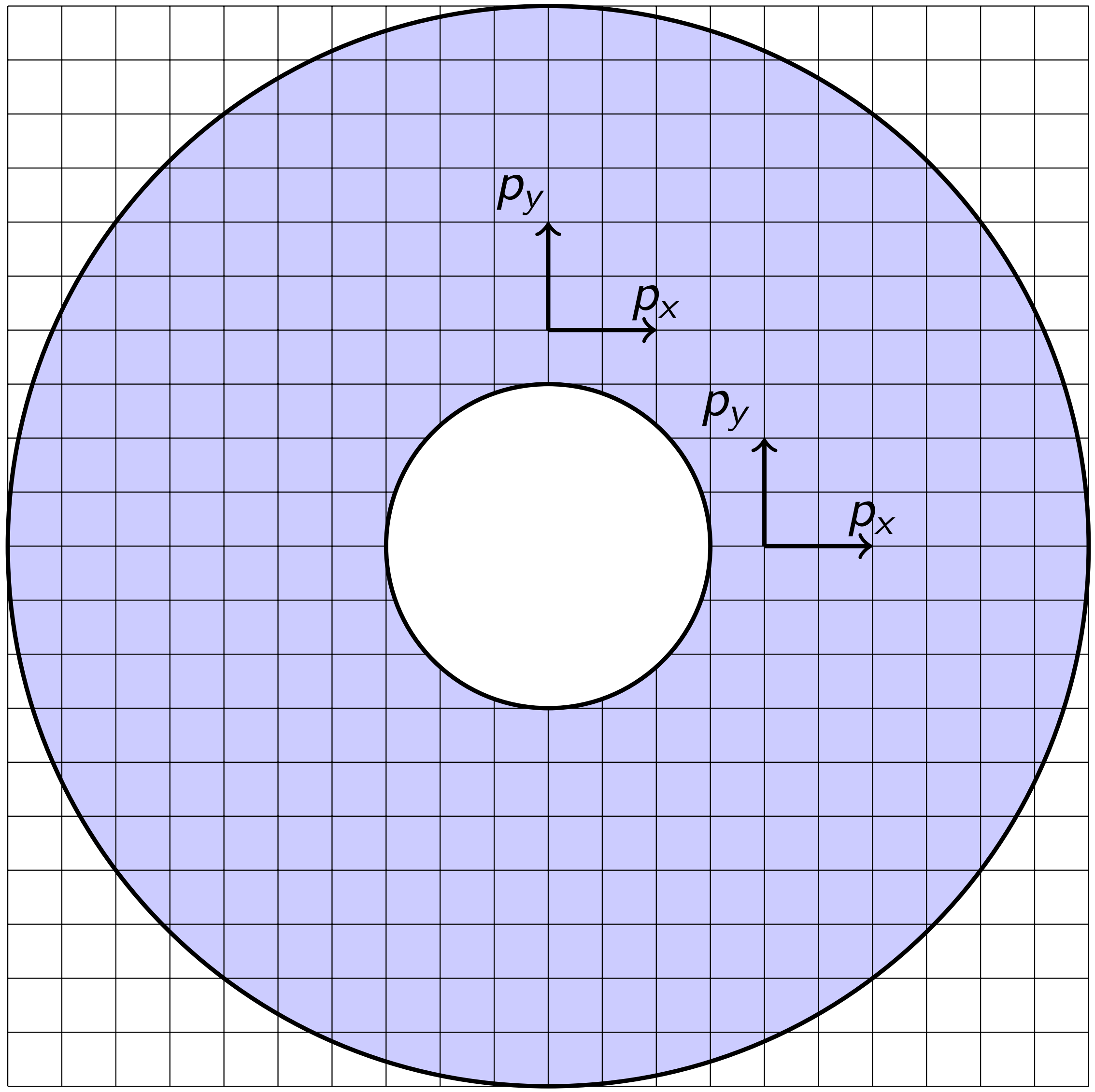

Boltzmann equation - arbitrary coordinates

- Consider a coordinate transformation $x^i \to x^{\widetilde{i}}$, which induces a metric $g_{\widetilde{\imath}\widetilde{\jmath}}$, as follows:

$$ds^2 = \delta_{ij} dx^i dx^j = g_{\widetilde{\imath}\widetilde{\jmath}} dx^{\widetilde{\imath}} dx^{\widetilde{\jmath}},$$

$$g_{\widetilde{\imath}\widetilde{\jmath}} = \delta_{ij} \frac{\partial x^i}{\partial x^{\widetilde{\imath}}} \frac{\partial x^j}{\partial x^{\widetilde{\jmath}}}.$$

- The Boltzmann equation with respect to the new spatial coordinates reads:

$$\frac{\partial f}{\partial t} + \frac{p^i}{m} \frac{\partial x^{\widetilde{\imath}}}{\partial x^i} \frac{\partial f}{\partial x^{\widetilde{\imath}}} + F^i \frac{\partial f}{\partial p^i} = J[f]. \tag{2}$$

Cylindrical grid and momentum space decomposition along the Cartesian axes

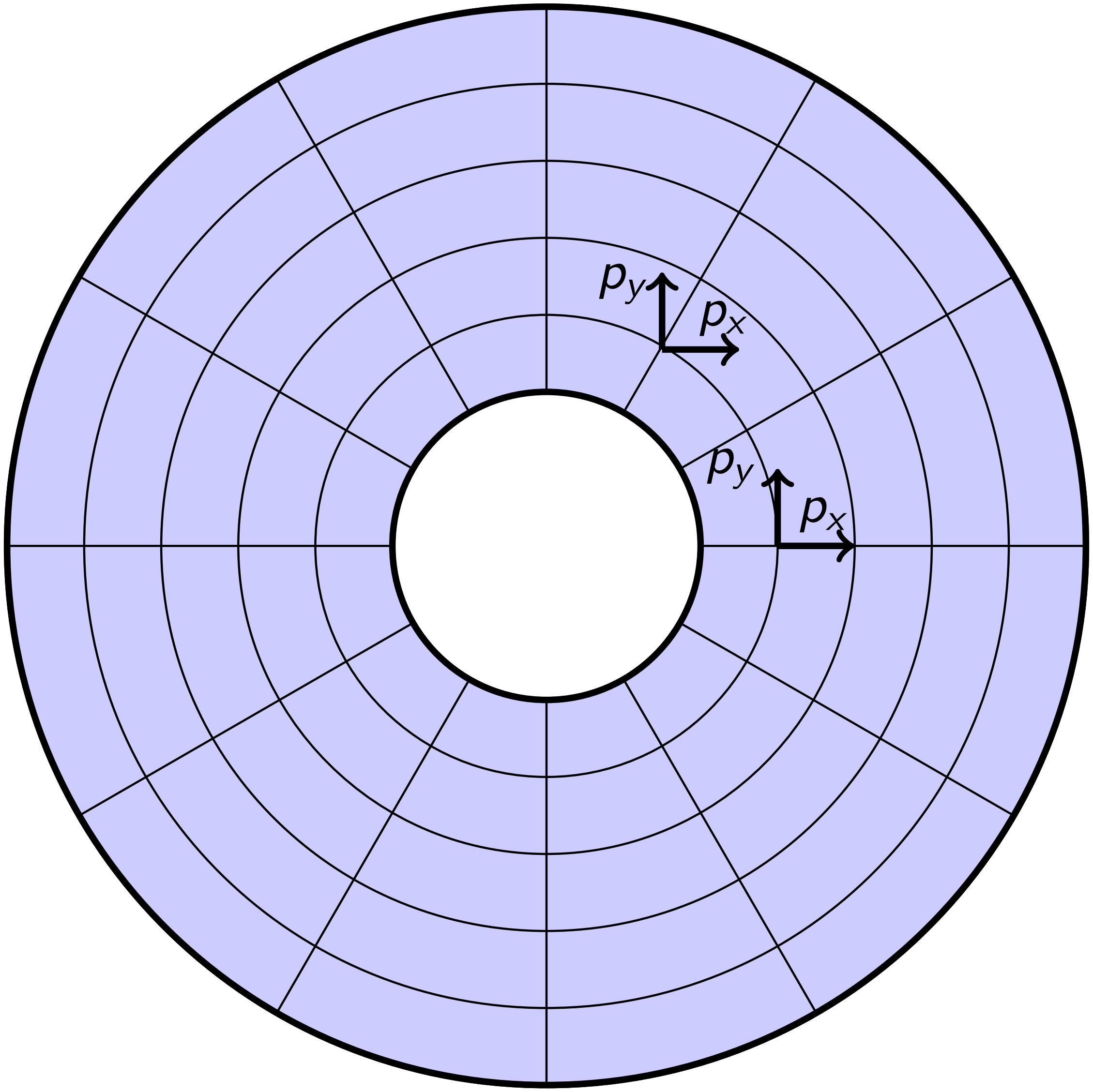

Boltzmann equation - orthonormal vielbein fields

- Furthermore, we note that:

$$p^{\widetilde{\imath}} = p^i \frac{\partial x^{\widetilde{\imath}}}{\partial x^i}, \qquad F^{\widetilde{\imath}} = F^i \frac{\partial x^{\widetilde{\imath}}}{\partial x^i}, \qquad \mathbf{p}^2 \equiv g_{\widetilde{\imath}\widetilde{\jmath}} p^{\widetilde{\imath}} p^{\widetilde{\jmath}}$$

- By introducing the triad vector frame and the associated one-form co-frame:

$$e_{\hat{a}} = e_{\hat{a}}^{\widetilde{\imath}} \partial_{\widetilde{\imath}}, \qquad \omega^{\hat{a}} = \omega^{\hat{a}}_{\widetilde{\imath}} dx^{\widetilde{\imath}}, \qquad g_{\widetilde{\imath}\widetilde{\jmath}} dx^{\widetilde{\imath}} dx^{\widetilde{\jmath}} = \delta_{\hat{a}\hat{b}} \omega^{\hat{a}} \omega^{\hat{b}}$$

  the inner product $\mathbf{p}^2 \equiv \delta_{\hat{a}\hat{b}} p^{\hat{a}} p^{\hat{b}}$ is decoupled from the metric.
- The Boltzmann equation reads:

$$\frac{\partial f}{\partial t} + \frac{p^{\hat{a}}}{m} e_{\hat{a}}^{\widetilde{\imath}} \frac{\partial f}{\partial x^{\widetilde{\imath}}} + \left(F^{\hat{a}} - \frac{1}{m} \Gamma^{\hat{a}}{}_{\hat{b}\hat{c}} p^{\hat{b}} p^{\hat{c}} \right) \frac{\partial f}{\partial p^{\hat{a}}} = J[f], \tag{3}$$

Cylindrical grid and momentum space decomposition adapted to the curvilinear coordinates.

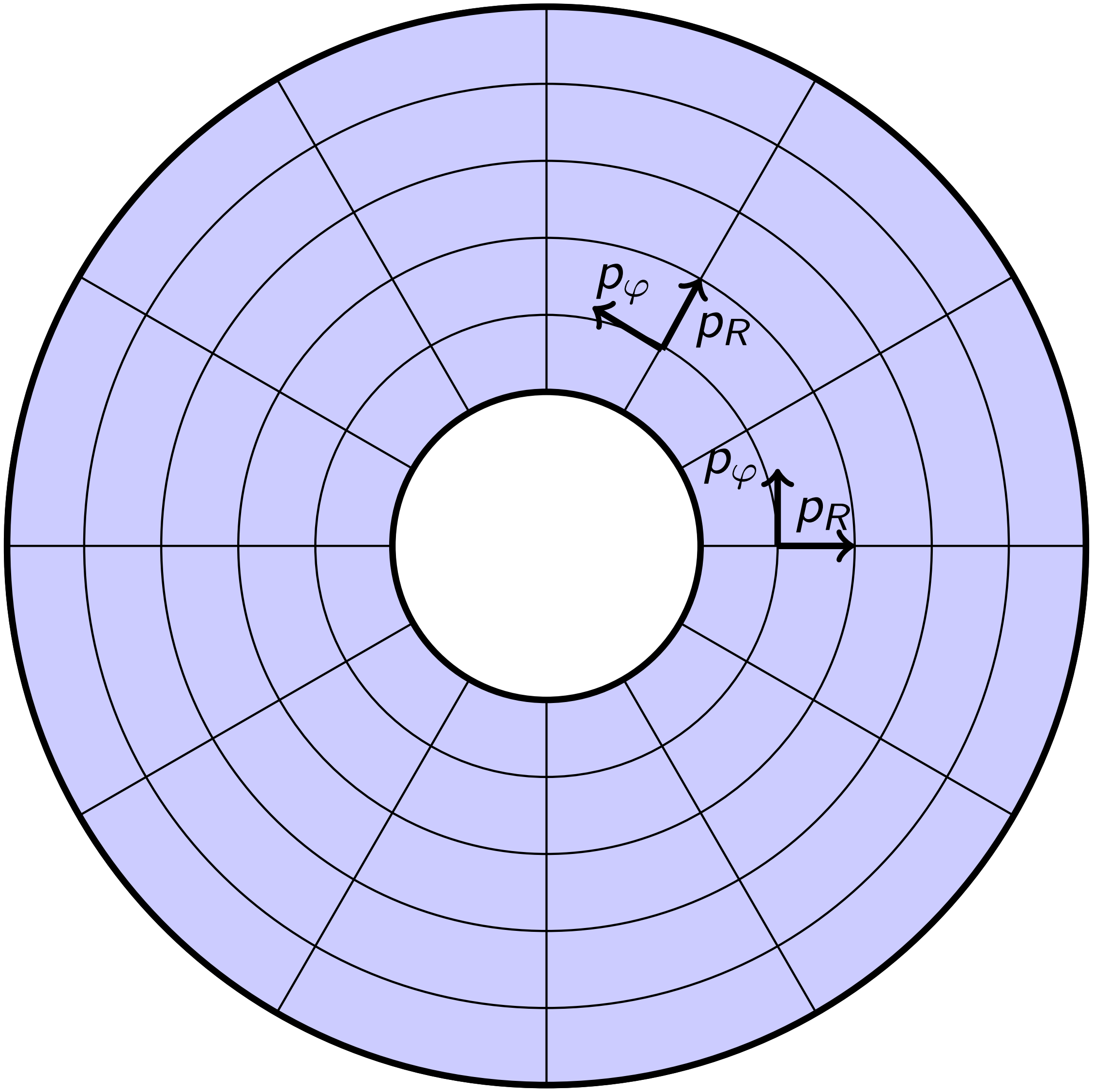

Cylindrical coordinates

- The line element in cylindrical coordinates and the associated triad are:

$$ds^2 = dR^2 + R^2 d\varphi^2 + dz^2, \qquad e_{\hat{R}} = \partial_R, \qquad e_{\hat{\varphi}} = R^{-1}\partial_\varphi, \qquad e_{\hat{z}} = \partial_z.$$

- The Boltzmann equation when the flow is homogeneous w.r.t. φ and z reads:

$$\frac{\partial f}{\partial t} + \frac{2p^{\hat{R}}}{m}\frac{\partial (fR)}{\partial R^2} + \frac{1}{mR}\left[(p^{\hat{\varphi}})^2 \frac{\partial f}{\partial p^{\hat{R}}} - p^{\hat{R}}\frac{\partial (f p^{\hat{\varphi}})}{\partial p^{\hat{\varphi}}}\right] = -\frac{1}{\tau}(f - f^{(\mathrm{eq})}). \qquad (4)$$

- The advection term is implemented following Falle et al.[1]

[1] S. A. E. G. Falle and S. S. Komissarov, Mon. Not. R. Astron. Soc. **278**, 586-602 (1996).

Coordinates streching

$$\text{Let } R(\eta) = R_{\rm in} + (R_{\rm out} - R_{\rm in})\left(\delta + \frac{A_0}{A}\tanh\eta\right), \qquad A_0 = \max(\delta, 1-\delta). \quad (5)$$

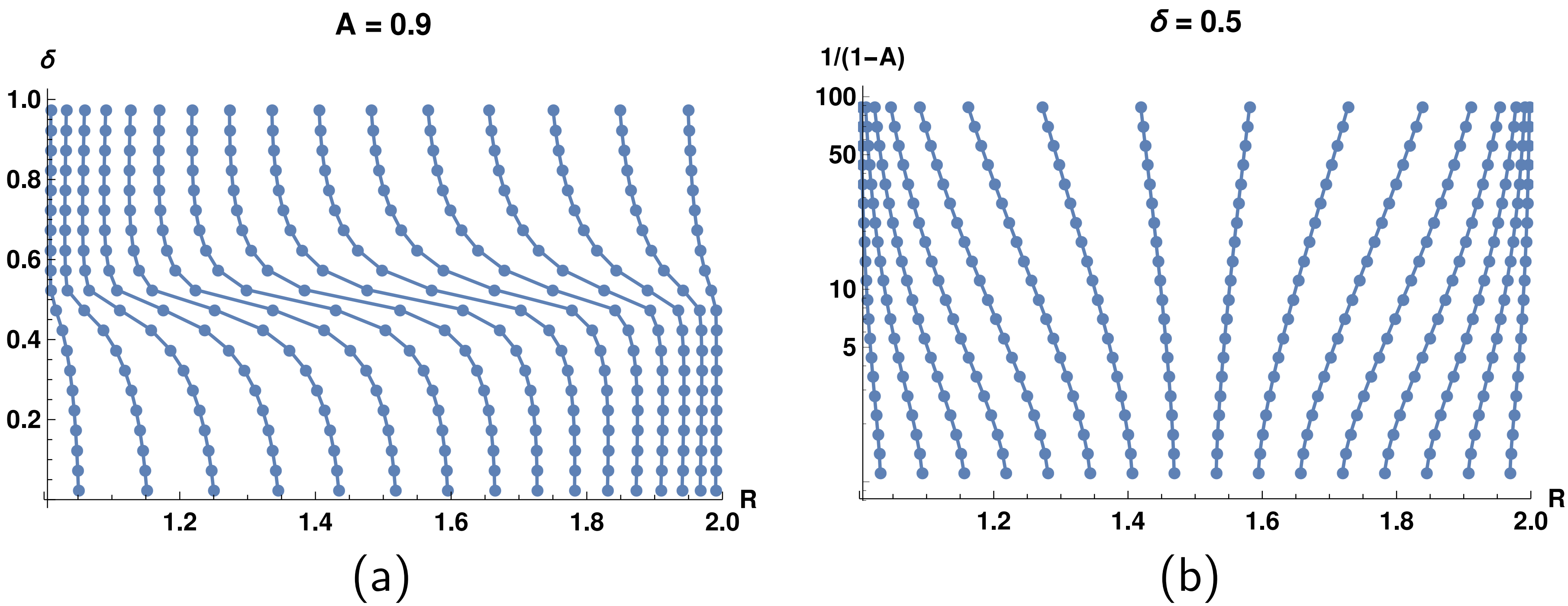

Figure: Effect of grid stretching on 16 points between $R_{\rm in} = 1$ and $R_{\rm out} = 2$.
(a) The parameter $\delta \in (0, 1)$ controls the positioning of the stretching centre.
(b) The parameter $A \in (0, 1)$ contains the amplitude of the stretching.
The points are equidistant in η.

Lattice Boltzmann - Gauss-Hermite quadratures

- The numerical models employed are mixed quadrature lattice Boltzmann[2]. f and $f^{(\rm eq)}$ are expanded with respect to Hermite(HLB) and Half-Range Hermite(HHLB) polynomials, e. g.(1D case):

$$f_i^{eq}(\mathbf{x}, t) = w_i \sum_{\ell=0}^{N} \frac{1}{\ell!} \mathbf{a}^{eq}_{(\ell)}(\mathbf{x}, t) \mathcal{H}^{(\ell)}(p_i)$$

- 3D model $=$ 1D $\times$ 1D $\times$ 1D.
- We will denote such models by: $\mathrm{HHLB}(Q_R) \times \mathrm{HLB}(\mathrm{Q}_\varphi) \times \mathrm{HLB}(Q_z)$.
- The moments of the distribution function are evaluated as:

$$\int d^3\hat{p}\, f\, p^{\hat{a}_1} \cdots p^{\hat{a}_s} = \sum_{i=1}^{\mathcal{Q}_R} \sum_{j=1}^{\mathcal{Q}_\varphi} \sum_{k=1}^{\mathcal{Q}_z} f_{ijk} \prod_{\ell=1}^{s} p_{ijk}^{\hat{a}_\ell}. \qquad (6)$$

Here $Q_\alpha, \alpha \in \{R, \varphi, z\}$ represents the quadrature order.

[2] V.E. Ambruș and V. Sofonea, J. Comput. Phys. **316**, 760-788 (2016)

Force term

Boltzmann equation written for the discrete distributions f_{ijk}:

$$\frac{\partial f_{ijk}}{\partial t} + \frac{2p_i^{\hat{R}}}{m} \frac{\partial (f_{ijk} R)}{\partial R^2} + \frac{1}{mR} \left\{ (p_j^{\hat{\varphi}})^2 \left(\frac{\partial f}{\partial p^{\hat{R}}} \right)_{ijk} - p_i^{\hat{R}} \left[\frac{\partial (f p^{\hat{\varphi}})}{\partial p^{\hat{\varphi}}} \right]_{ijk} \right\} = -\frac{1}{\tau}(f_{ijk} - f_{ijk}^{(\mathrm{eq})})$$

- We write the terms involving the derivative of f as follows[3] :

$$\left(\frac{\partial f}{\partial p^{\hat{R}}} \right)_{ijk} = \sum_{i'=1}^{\mathcal{Q}_R} \mathcal{F}^R_{i,i'} f_{i'jk},$$

- The matrix $\mathcal{F}^R_{k,j}$ has the following form:

$$\mathcal{F}^R_{k,j} = -w_k^H \sum_{\ell=0}^{Q-1} \frac{1}{\ell!} H_{\ell+1}(p_k) H_\ell(p_j)$$

[3] V. E. Ambruș, V. Sofonea, R. Fournier, and S. Blanco, *Implementation of the force term in half-range lattice Boltzmann models*, in preparation.

Lattice Boltzmann - Numerical scheme

- Velocity vectors are given by the roots of the Hermite/Half-Range Hermite polynomials.
- The roots are irrational numbers for a quadrature order $Q > 2$ which implies a off-lattice velocity set.
- Time-stepping: TVD RK3[4]
- Advection: The fifth order WENO-5 scheme[5].

[4] C.-W. Shu and S. Osher, J. Comput. Phys. 77, 439–471 (1988).
[5] G. S. Jiang and C. W. Shu, J. Comput. Phys. 126, 202 (1996).

Diffuse reflection boundary conditions

- Reflected particles carry some information that belongs to the wall.

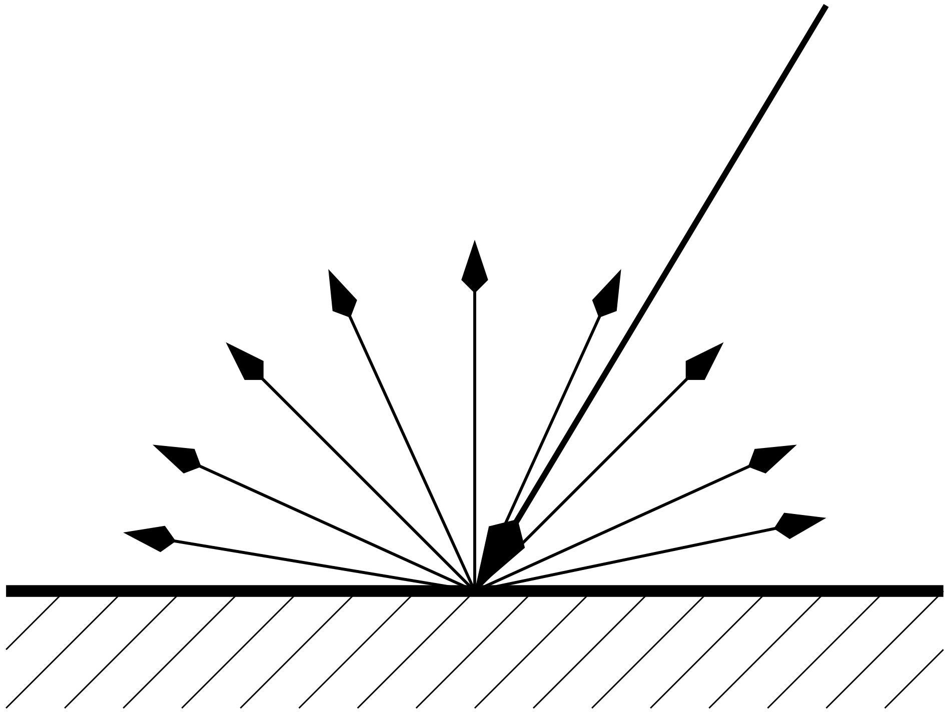

diffuse reflection

- The density $n_{\rm w}$ is fixed by imposing zero flux through the boundary:

$$\int_{\mathbf{p}\cdot\chi>0} d^3p\, f\,(\mathbf{p}\cdot\chi) = -\int_{\mathbf{p}\cdot\chi<0} d^3p\, f^{(\rm eq)}\,(\mathbf{p}\cdot\chi).$$

Circular Couette flow

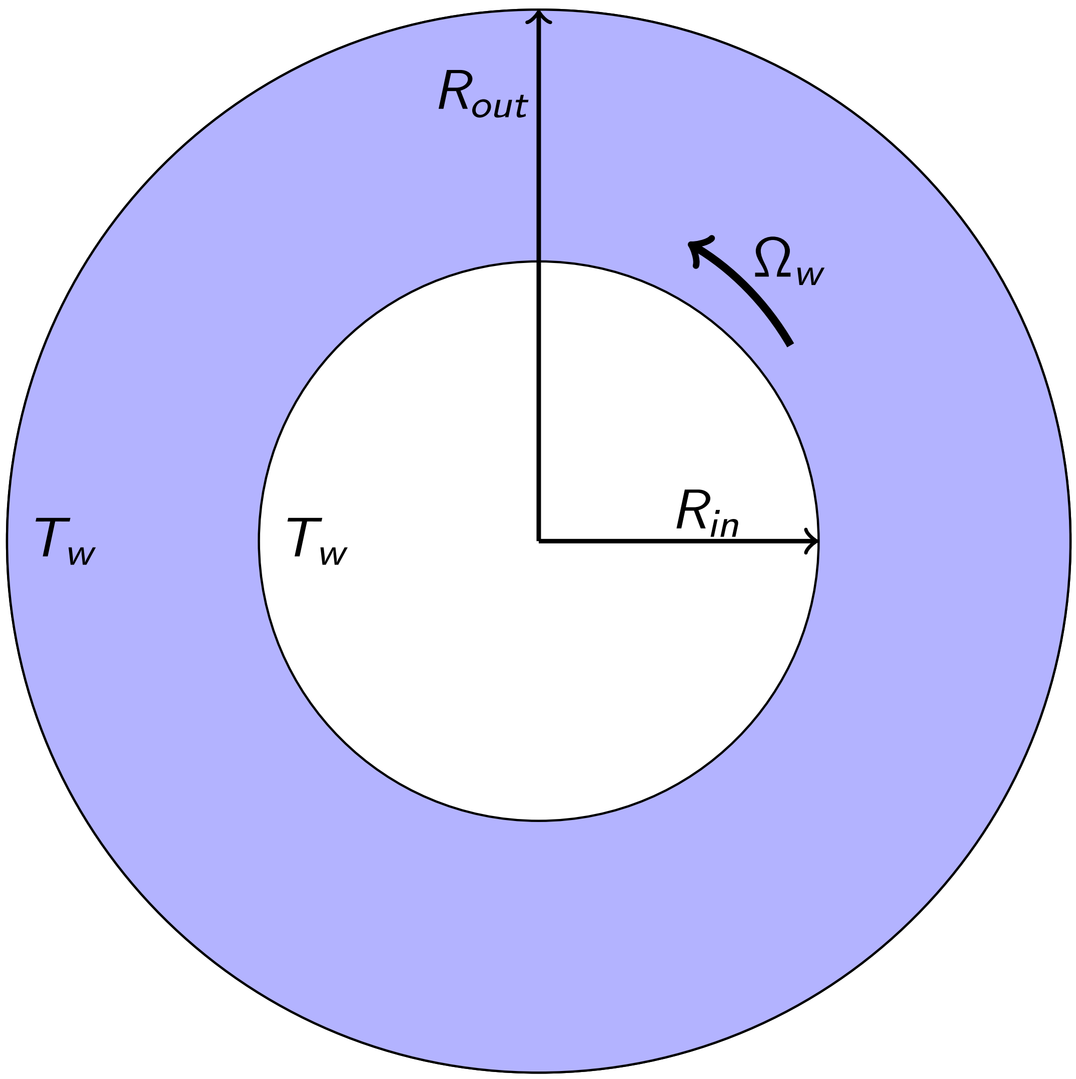

Knudsen number $Kn = \lambda/L$.

Rigid rotation

- Angular speed $\Omega_{\rm in} = \Omega_{\rm out} = \Omega_w$, $T_{\rm in} = T_{\rm out} = T_w$, the analytic solution of the Boltzmann equation reads:

$$f(R) = \frac{n(R)}{(2\pi m T_w)^{3/2}} \exp\left[-\frac{p_{\hat{R}}^2 + (p_{\hat{\varphi}} - \Omega R)^2 + p_{\hat{z}}^2}{2mT_w}\right], \tag{7}$$

where $n(R)$ is given by [6]:

$$n(R) = \frac{N}{H}\frac{m\Omega^2}{4\pi T_w}\frac{\exp\left[\frac{m\Omega^2}{4T_w}(2R^2 - R_1^2 - R_2^2)\right]}{\sinh\left[\frac{m\Omega^2}{4T_w}(R_2^2 - R_1^2)\right]}. \tag{8}$$

- Eq. (7) satisfies the Boltzmann equation for all values of the relaxation time.

[6] L. M. G. Cumin, G. M. Kremer, and F. Sharipov, Math. Mod. Meth. App. S. **12**, 445–459 (2002).

Rigid rotation

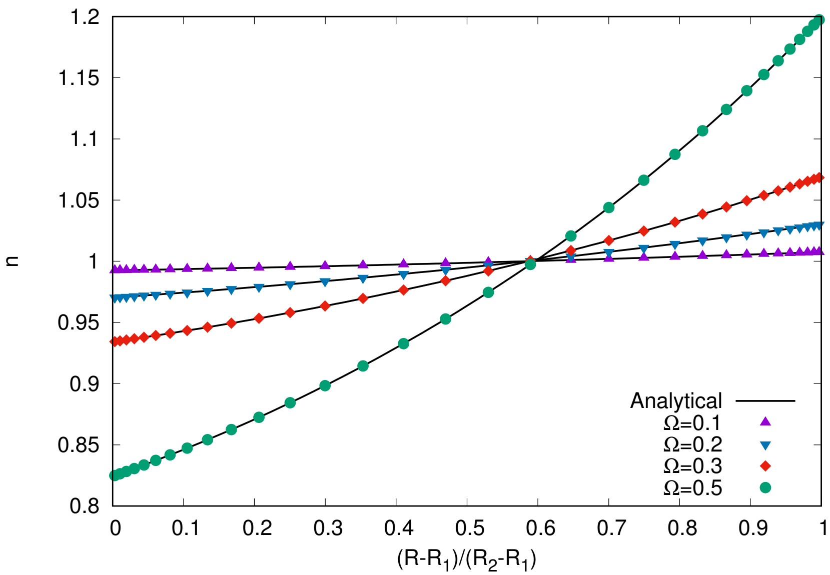

(a)

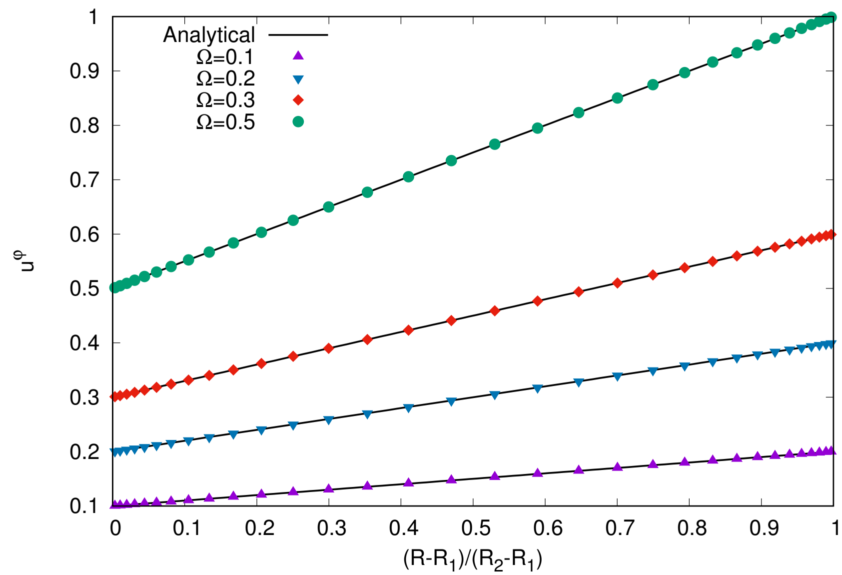

(b)

Figure: Comparison of simulation results with analytic solutions for results:
(a) Density profile ;
(b) Azimuthal velocity;
obtained using the $\mathrm{HLB}(4) \times \mathrm{HLB}(4) \times \mathrm{HLB}(2)$ models and $N_R = 32$ nodes.

Hydrodynamic flow regime - $Kn \to 0$

- Number density is evaluated by numerically solving:

$$\partial_R \ln P = \frac{(u^{\hat{\varphi}})^2}{RT}. \tag{9}$$

where $n = P/T$ and by using the constraint $2\pi \int_{R_{\rm in}}^{R_{\rm out}} nRdR = N_{\rm tot}$.

- Azimuthal velocity:

$$u^{\hat{\varphi}} = R^{-1}\frac{\Omega_{\rm in}}{R_{\rm in}^{-2} - R_{\rm out}^{-2}} - R\frac{\Omega_{\rm in} R_{\rm in}^2}{R_{\rm out}^2 - R_{\rm in}^2}, \tag{10}$$

- Temperature:

$$T = T_w + \frac{\eta}{\kappa}\frac{\Omega_{\rm in}^2}{R_{\rm in}^{-2} - R_{\rm out}^{-2}} \times \left(\frac{R_{\rm in}^{-2} - R^{-2}}{R_{\rm in}^{-2} - R_{\rm out}^{-2}} - \frac{\ln(R/R_{\rm in})}{\ln(R_{\rm out}/R_{\rm in})}\right) \tag{11}$$

- Radial heat flux:

$$q^{\hat{R}} = -\frac{\eta}{R}\frac{\Omega_{\rm in}^2}{R_{\rm in}^{-2} - R_{\rm out}^{-2}} \times \left[\frac{2R^{-2}}{R_{\rm in}^{-2} - R_{\rm out}^{-2}} - \frac{1}{\ln(R_{\rm out}/R_{\rm in})}\right]. \tag{12}$$

Low Mach flows

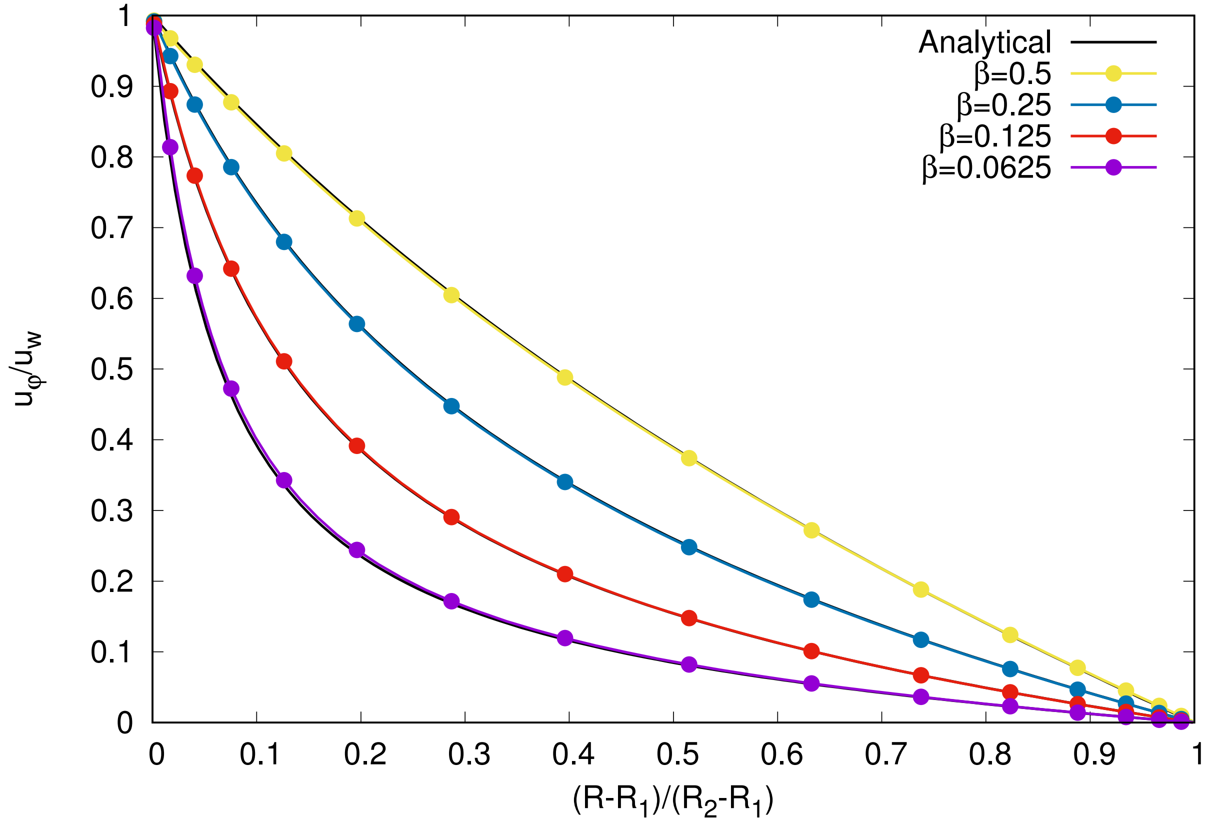

Figure: $u^\varphi(R)/u_w$ profile, where $u^\varphi = \Omega R$, $\Omega_{\rm in} = 0.01$, $\beta = R_{\rm in}/R_{\rm out}$. Numerical results obtained using $\mathrm{HLB}(3) \times \mathrm{HLB}(3) \times \mathrm{HLB}(2)$ models and $N_R = 64$ nodes.

Non-negligible Mach flows

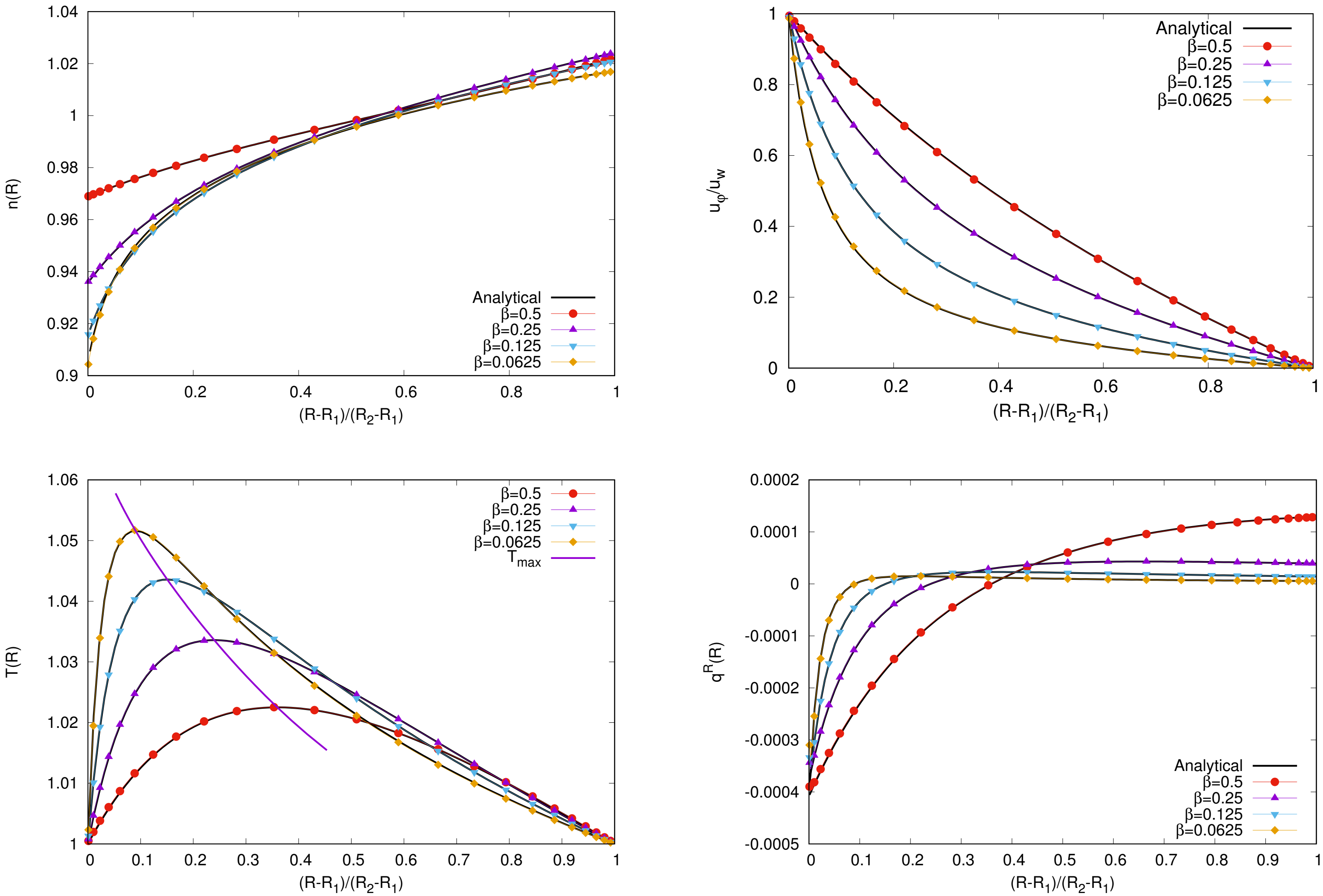

Figure: Comparison between the numerical and analytic results for the profiles of (a) $n(R)$; (b) $u^{\varphi}(R)/u_w$; (c) $T(R)$; (d) $q^{\hat{R}}(R)$. $\beta = R_{\rm in}/R_{\rm out}$, $\Omega_{\rm in} = 0.5$. Numerical results obtained using $\mathrm{HLB}(5) \times \mathrm{HLB}(5) \times \mathrm{HLB}(3)$ models and $N_R = 96$ nodes.

Radial heat flux

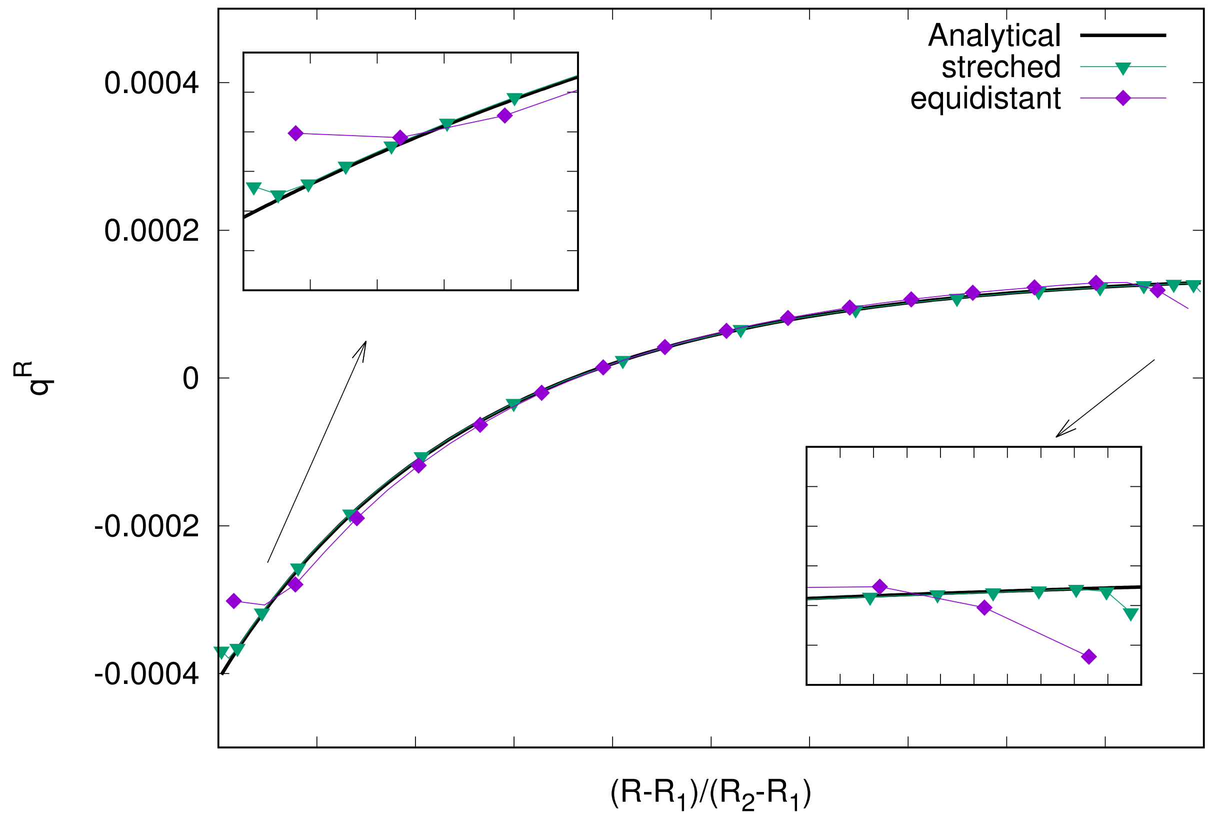

Figure: Comparison streched and equidistant spatial discretisation with the same number of lattice nodes $N_R = 32$.

Transition flow regime

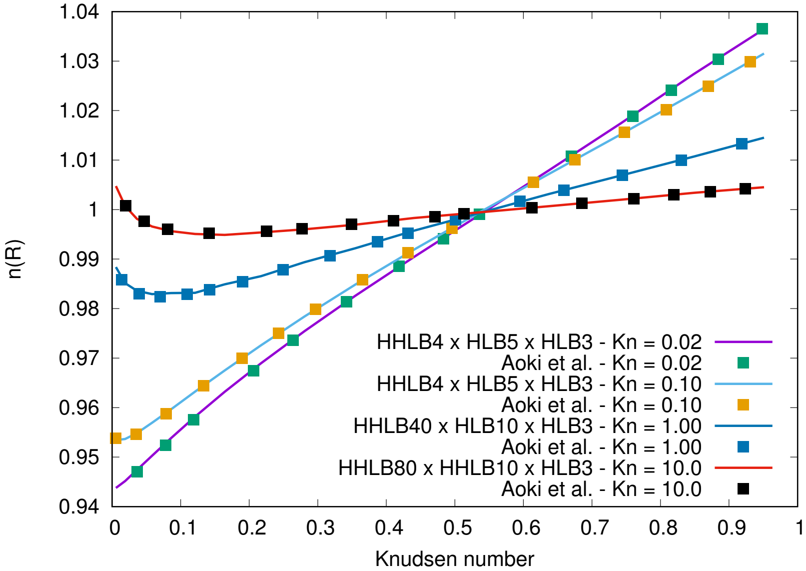

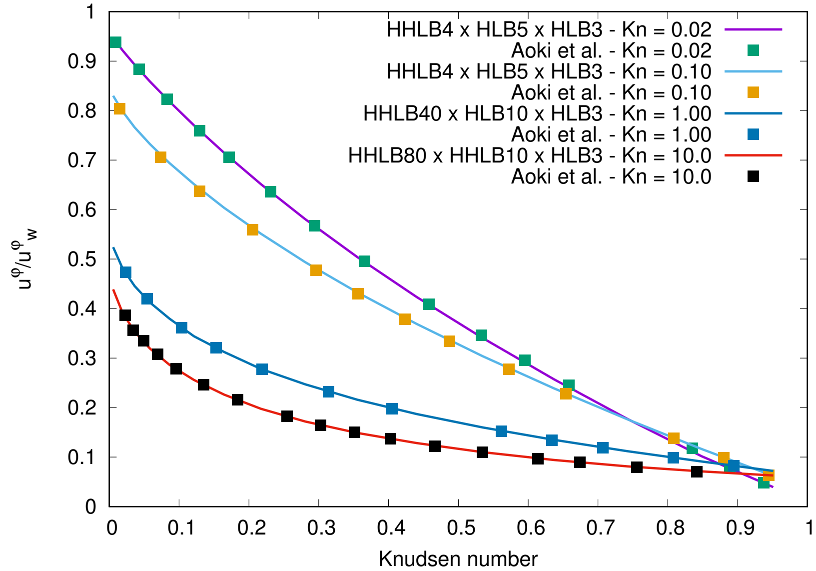

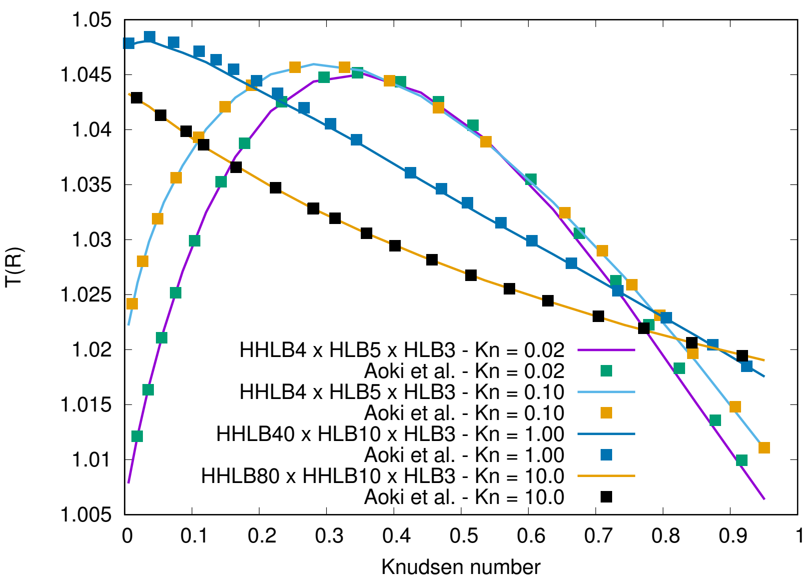

Comparison between our simulation results and those reported by Aoki et al.[5]: $n(R)$; $T(R)$; $u^{\hat{\varphi}}(R)/u^{\varphi}_w$, $\Omega_{\rm in} = 0.5\sqrt{2}$ and $N_R = 16$ nodes.

[6]K. Aoki, H. Yoshida, T. Nakanishi, and A. L. Garcia, Phys. Rev. E 68, 016302 (2003).

Free molecular flow regime - $Kn \to \infty$

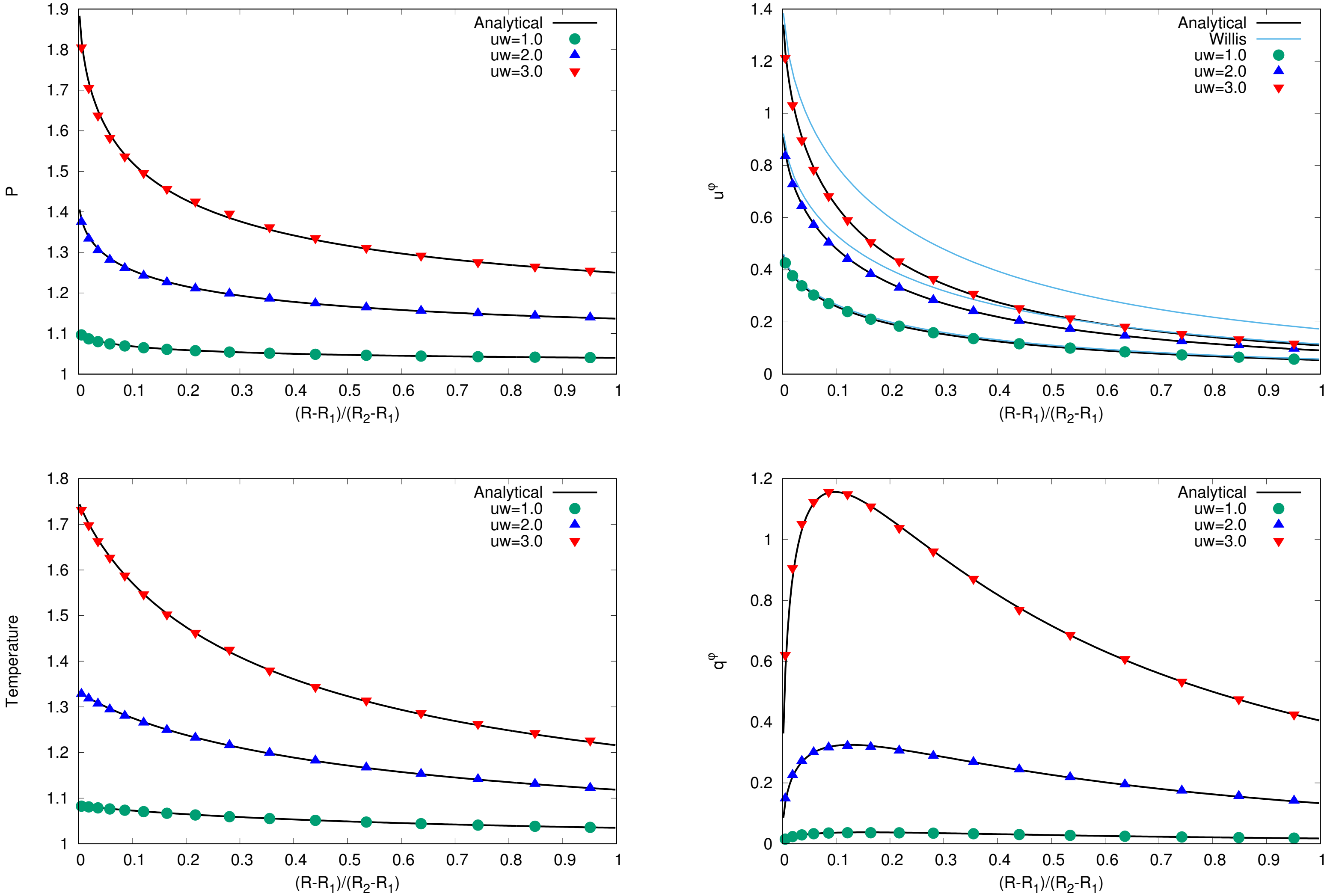

Figure: Comparison between our numerical results and the analytic predictions in the ballistic regime. (a) $P = n \cdot T$; (b) $u^{\hat{\varphi}}$; (c) T; (d) $q^{\hat{\varphi}}$. The HHLB(200) $\times$ HHLB(10) $\times$ HLB(3) model and $N_R = 16$ nodes. The analytic solution for $u^{\hat{\varphi}}$ reported by Willis[8] is shown in (b) alongside our analytic expressions.

[8] D. R. Willis, Phys. Fluids 8, 1908 (1965)

Conclusion

- We introduced the Boltzmann equation written with respect to orthogonal vielbeins.
- The vielbeins allow the decoupling between the momentum space and the coordinate space, i.e. $\mathbf{p}^2$ is coordinate-independent.
- The vielbein permits the momentum space degrees of freedom to be aligned according to the symmetries of the flow.
- We considered the shear flow between two coaxial cylinders(circular Couette flow) which becomes one-dimensional in space since the vielbein allows the symmetry of the geometry to be transferred to the momentum space.
- Our models give accurate results throughout the whole range of Kn.

Thank you for your attention.

This work was supported by a grant from the Romanian National Authority for Scientific Research and Innovation, CNCS-UEFISCDI, project number PN-II-RU-TE-2014-4-2910.